Supporting Online Material

Materials and methods

Except were otherwise stated, all samples were taken from the Iceman's body with minimal contamination in September 2000 while the first author was present, and subsequently stored in acid-cleaned teflon vials. Tooth samples of the permanent dentition include five milligram-sized enamel fragments and one composite enamel-dentine piece (Fig. 2C) of three teeth (canine, 1st and 2nd premolar), all from the right maxilla. Bone samples from the femur (both cortical and trabecular) are the same as used for radiocarbon dating (619/91/Z2KN, ETH-8342; taken in 1991), and were provided by G. Bonani (ETH Zürich) (*S1, S2*). The sample of intestine content is from the terminal ileum. Samples of the Iceman's equipment obtained from K. Oeggl (Univ. Innsbruck, Austria; (*S3*)) included mg-sized pieces of larch wood from the backpack (92/400) and lime bast (92/402b); sample numbers are from (*S4*)). Two mg-sized fragments of the Iceman's clothing made from goat fur (*S5*) were obtained from K. Spindler (Univ. Innsbruck, Austria; UF:0/1, UF:0/2); due to their small size they cannot be compared to the rest of the clothing. Ice cores from the Iceman's site drilled in 1992 (see (*S4*) for details and sample numbers) were obtained from S. Bortenschlager (Univ. Innsbruck, Austria), and were used to assess post-mortem alteration of the trace elemental and isotopic signatures of the Iceman samples (Tabs. S1, S2). Soil samples from Neolithic – Copper age archaeological horizons that minimize the risk of deriving an anthropogenically modified signal (particularly crucial for Pb) were provided by the Cultural Heritage Office in Bolzano (L. dal Ri) for comparison with the radiogenic isotopic composition of the Iceman. In order to provide a framework for interpreting oxygen isotope ratios of the Iceman's biominerals, several rivers were sampled in both northern and southern valleys at elevation intervals of 250-500 m during late June and late September 2001 and June 2002, and analyzed for their oxygen isotopic composition. (Fig. 1; Tab. S1). Local springs and small streams were sampled as well. Third molars of the local present-day human population (for details see Tab. S1a) were obtained from two dentists through E. Egarter Vigl (Bolzano), in order to prepare tooth enamel for oxygen isotope ratio analysis.

Before cleaning and dissolution, tooth fragments were imaged using a Hitachi S2250-N Scanning Electron Microscope with 90 μA emission current. Dentine and enamel of the small

canine fragment (inset in Fig. 2C) were separated along a pre-existing crack using a small chisel. Using laser-ablation ICPMS, both freshly-broken and outer surfaces of enamel as well as cross-sections of dentine – enamel (inset in Fig. 2C) were analyzed for trace elemental concentrations ((*S6*); see (*S7*) for methodological details). Before dissolution, all tooth and bone samples were repeatedly ultrasonically cleaned in ethanol, teflon-distilled acetone and high-purity Milli-Q water, dried and subsequently weighed.

Oxygen and carbon isotopic analysis

Prior to stable isotope analysis, tooth enamel fragments were ground in a mortar and pestle. Resulting powders were then soaked for 24 hours in 1M acetic acid to remove any carbonate contaminants, rinsed 5 times with distilled water, and then dried. Prior to treatment in acetic acid, bone samples were soaked in 3% NaOCl for 24 hours. All samples were analyzed on a Finnigan MAT 252 Isotope Ratio Mass Spectrometer with a Kiel III automated carbonate device housed in the Paul H. Nelson Stable Isotope Laboratory at the University of Iowa. Daily analysis of powdered carbonate standards (NBS-18 and NBS-19) and several in-house standards were conducted. Analytical precision on these standards was better than ± 0.1‰ for $\delta^{18}O$ and $\delta^{13}C$. Oxygen and carbon isotope results of biominerals (carbonate component) are reported in per mil (‰) relative to V-PDB (Tab. S1).

Water samples were kept refrigerated in Nalgene bottles. These samples were analyzed using a Micromass SIRA Series II Dual Inlet mass spectrometer with a custom CO_2/H_2O equilibration system in the Stable Isotope Laboratory of the Institute of Arctic and Alpine Research, University of Colorado. Typical reproducibility between multiple standards in one set of samples is ±0.06 for $\delta^{18}O$. All oxygen isotope results of waters are reported in per mil (‰) relative to V-SMOW (Tab. S1).

Sr-Pb isotopic analysis

All tooth fragments were separately analyzed for their Sr isotopic composition (Tab. S2a). In view of the low Pb concentation (0.12 ppm), however, the dissolutions of the two largest enamel fragments were analyzed together for Pb isotopes in order to achieve reasonable precision (Tab. S2b). No Pb isotope data are available for the two small enamel pieces. Sr (and Pb) isotopic analysis of all biominerals samples was conducted in three leaching/dissolution steps with

sequentially stronger acids. The rationale is that post-mortem alteration becomes predominantly evident in the first leaching steps, which preferentially dissolve adsorbed or least strongly bound and most easily diagenetically-affected parts (*S8*). Samples were leached in 3 ml closed teflon vials with ultrasonic agitation using 500 µl 0.1M acetic acid for 1 hour (leach L1), and 500 µl 1M acetic acid for 24 hours (leach L2), including two rinses with 200 µl H_2O each, which were combined with the respective leach. Subsequent dissolution (wet-ashing) was performed in 3 ml closed teflon vials overnight in one or two steps using 500 µl 7.9M HNO_3 each. The leachates and dissolved samples were spiked with an ^{84}Sr tracer, or aliquotted followed by adding ^{84}Sr and ^{208}Pb tracers (Z2KN1, Z2KN2, 4lg1). Sr and Pb were sequentially separated using miniature extraction chromatographic colums with a stratified resin bed of 25 µl Prefilter resin (bottom) and 25 µl SrSpec resin (top) (modified from (*S9-S11*)). H_2O and 6M HCl were used as eluting agents for Sr and Pb, respectively. Pb (and sometimes also Sr) was purified twice using the same ion exchange column. Procedure blanks ranged between 5.4 – 28.0 pg Sr ($^{87}Sr/^{86}Sr$ = 0.7097 ± 0.0020; 1 S.D.) and 13.4 – 26.7 pg Pb ($^{206}Pb/^{204}Pb$ = 18.259 ± 0.015, $^{207}Pb/^{206}Pb$ = 0.85602 ± 0.00034, $^{208}Pb/^{206}Pb$ = 2.0992 ± 0.0010; all 1 S.D.); only the smallest Sr analyses and all Pb analyses of the biominerals have been corrected for analytical blank. After leaching with 1200 µl 2M HCl for ~2 hours and an associated H_2O-rinse, all organic samples (wood, fur, and intestine contents) were repeatedly (up to 4 times) wet-ashed in closed 3 ml teflon vials using 500 µl 7.9M HNO_3, followed by addition of a ^{84}Sr tracer, and a final equilibration step with $HClO_4$ and HNO_3. Sr was purified using the same Prefilter-SrSpec extraction chromatographic setup as used for biominerals. Soils leachates were used in order to extract the biologically available fraction of trace elements only from soil samples, which becomes incorporated in biogenic apatite through nutrition. Two grams of soil were leached in 8 ml 2M acetic acid in closed teflon vials with regular ultrasonic agitation for one week. After centrifuging, the supernatant was pipetted off, dried down and re-equilibrated with 7.9M HNO_3. Sr and Pb was purified using Prefilter-SrSpec extraction chromatography.

All Sr isotopic compositions and Sr concentrations were measured using a TRITON thermal-ionization multi-collector mass-spectrometer (TIMS) at the Research School of Earth Sciences (RSES, ANU) in static Faraday mode following loading with a Ta-emitter solution onto zone-refined outgassed Re-filaments (*S12*). Analyses of the NIST SRM987 Sr standard (50 ng) over the course of the measurements yielded 0.710281 ± 0.000017 for an earlier, and 0.710219 ±

0.000013 (both 2 S.D.) for a later period, respectively. This change was induced by some hardware modifications on the TRITON TIMS. All Sr isotopic analyses were adjusted to the adopted value of 0.710245 for the NIST SRM987 standard. Errors (95% c.l.) include the combined error of each individual analysis and the reproducibility of the standard. Pb separated from biominerals was loaded onto zone-refined outgassed Re filaments using Si-Gel (*S13*); the isotopic compositions and concentrations were measured separately on the TRITON mass-spectrometer with strict adherence to a temperature interval of 1180 – 1200ºC. Whenever possible, analyses were performed in static mode (Faraday) with ^{204}Pb measured on a secondary electron-multiplier (SEM) operated in ion-counting mode. Alternatively, all Pb-isotopes were measured in dynamic mode using the SEM. Pb isotopic analyses were corrected for mass spectrometric fractionation on the basis of repeated analyses of the NIST SRM981 Pb standard (1-2 ng) by 0.000822 ± 0.000061 (1 S.D.) per amu. Corresponding errors are 1.37 ‰, 0.66‰, and 3.16 ‰ for ^{208}Pb/^{206}Pb, ^{207}Pb/^{206}Pb, and ^{206}Pb/^{204}Pb, respectively, and were propagated into the final errors for the Pb analysis of the biominerals given at 95% c.l. The Pb isotopic composition of soil leachates was analyzed using a multi-collector inductively-coupled-plasma mass spectrometer (MC-ICPMS, NEPTUNE) at the Research School of Earth Sciences (RSES, ANU) using NIST SRM997 Tl to correct for mass bias, after adding appropriate amounts of Tl to samples to ensure a Pb/Tl ratio of ~12.5 in the samples. Samples were introduced into the MC-ICPMS using a standard ES-2101 quartz-glass spray chamber with a PFA 50 µl/min nebulizer. Using a constant ^{205}Tl/^{203}Tl ratio of 2.3885, repeated measurements of the NIST SRM981 Pb standard yielded values of ^{208}Pb/^{206}Pb = 2.16751, ^{207}Pb/^{206}Pb = 0.914813, and ^{206}Pb/^{204}Pb = 16.9406, with 60.6, 31.6, and 92.0 ppm (2 S.D.) external reproducibility, respectively. TIMS and MC-ICPMS Pb data were adjusted to the NIST SRM981 standard values given by (*S14*). Constants used are those from (*S15*).

^{40}Ar-^{39}Ar experimental techniques

The 12 intestine mica grains were carefully cleaned in acetone, methanol, and deionised water. The grains were wrapped in aluminium foil and loaded into an aluminium package containing other samples for neutron irradiation. Biotite age standards Tinto B (K-Ar age of 409.24 ± 0.71 Ma (*S16*) and HD-B1 (K-Ar age of 24.21 ± 0.32 Ma (*S17*)) was loaded at ca. 5 mm intervals along the package to monitor the neutron flux gradient. The packages were Cd-shielded and fast

neutron irradiated in the 5C position of the McMaster University Nuclear Reactor (Canada) for 20 hours. Principles of the ^{40}Ar-^{39}Ar technique can be found in (*S18, S19*).

Upon return, the samples were loaded into an ultra-high vacuum laser chamber with a Kovar viewport and baked to 120°C overnight to remove adsorbed atmospheric argon from the samples and chamber walls. A 110 W Spectron Laser Systems continuous-wave Nd-YAG 1064 nm laser, was used to totally fuse the individual mica grains. The Ar isotopes were measured using a high sensitivity MAP 215-50 mass spectrometer fitted with a Balzers SEV 217 multiplier. The ^{40}Ar/^{39}Ar data presented in this study were undertaken at the Western Australian Argon Isotope Facility, operated by a consortium of Curtin University and University of Western Australia. The mean extraction system blank Ar isotope measurements obtained during the analyses were 2.1×10^{-12}, 6.9×10^{-15}, 3.9×10^{-15}, 8.6×10^{-14}, and 2.4×10^{-14} cm^3 STP for ^{40}Ar, ^{39}Ar, ^{38}Ar, ^{37}Ar, and ^{36}Ar respectively. Ar analyses were corrected for extraction line blanks, mass spectrometer discrimination, and nuclear interference reactions (Tab. S3). Errors quoted on the ages are 1 sigma, and ^{40}Ar/^{39}Ar ages were calculated using the decay constant in (*S15*).

Supporting text

Using a slightly different calibration (*S20*) does not change any of the conclusions drawn here. In fact, even heavier δ^{18}O values of water are calculated from the Iceman's and present-day human biominerals for the period of their mineralization.

A minimum water volume (^{87}Sr/^{86}Sr = 0.727, Sr_{conc} = 2 ppb; Tab. S2a - ice cores) of ~1500-1700-times that of bone is required to have fully exchanged with bone. In reality, the water(ice)-bone ratio will be significantly greater because of the lower partitioning for Sr between biogenic apatite and water, but the lack of information about partition coefficients for Sr does not allow a more detailed assessment.

Whereas ice cores closest to the Iceman have high ^{87}Sr/^{86}Sr ratios of 0.723-0.729, other ice cores more than 2 m away also show lower ^{87}Sr/^{86}Sr ratios between 0.717-0.720 (Tab. S2a). These variations in Sr isotopic ratios in ice cores at the Iceman site argue against later large-scale melting of ice after trapping of the body. This scenario has been invoked (*S21*) to explain the skin alteration and the distribution of artefacts at the Iceman's site. In such a case, however, Sr

isotopes in ice are expected be more homogenous, which is not the case. Therefore, a meltwater pool is more likely to have existed only shortly after the Iceman´s death.

Much smaller white micas are also found in the lung (*S22*). Their grain sizes are mostly only tenths of μm, and only occasionally a few μm. However, even the latter size is too small for $^{40}Ar/^{39}Ar$ dating of individual mica grains.

Using trace elemental ratios in the Iceman's bones (*S23*) is unreliable given the documented alteration of the Iceman's bones due to interaction with melt water (*S24*), and of soil-buried bones in general (*S25*). Moreover, even if the pristine trace elemental signature was preserved in those bones, it remains unclear how well similar lithologies north and south of the Alpine watershed (predominantly gneisses and micaschists, Fig. 1) can be distinguished on the basis of trace elemental ratios. Lastly, the $\delta^{18}O$ dataset of medieval bones (*S23*) used for comparison with the Iceman's bones is highly variable even for a single location (e.g. Naturns: (*S23*)), which impedes a conclusive comparison with the respective data of the Iceman.

Fig. 1 was based on the map by Bigi et al. (*S26*), and modified using information from the following references: (*S27-S40*).

Supporting figures

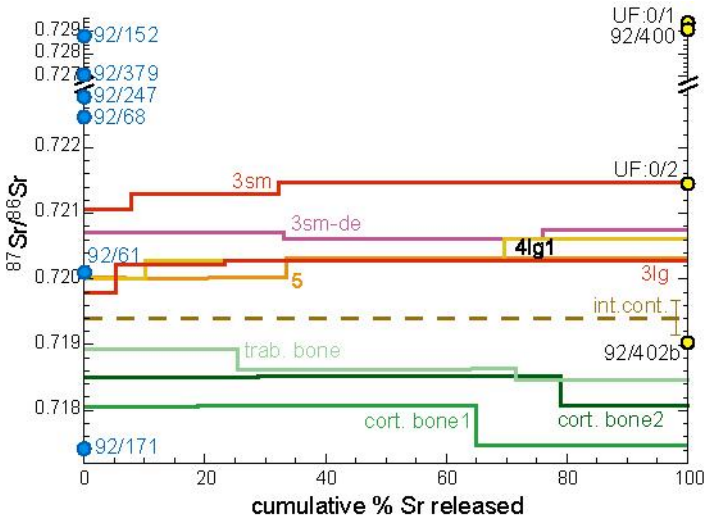

Fig. S1: $^{87}Sr/^{86}Sr$ ratio of the Iceman's biominerals plotted against cumulative percentage of Sr released in three leaching/dissolution steps. The Sr isotopic composition of the intestinal content is marked as dashed line. Corresponding results for ice cores and the Iceman's equipment are given as blue and yellow-black dots on the left and right y-axes, respectively; see Tab. S2a and (*S2, S4*) for respective sample identifiers. Error bars are smaller that the line thickness or the plot symbol, except where indicated. Abbreviations: 3…canine-enamel, 4…1st premolar-enamel, 5…2nd premolar-enamel, 3de…canine-dentine; sm…small, lg…large; int.cont…intestine content, trab…trabecular, cort…cortical.

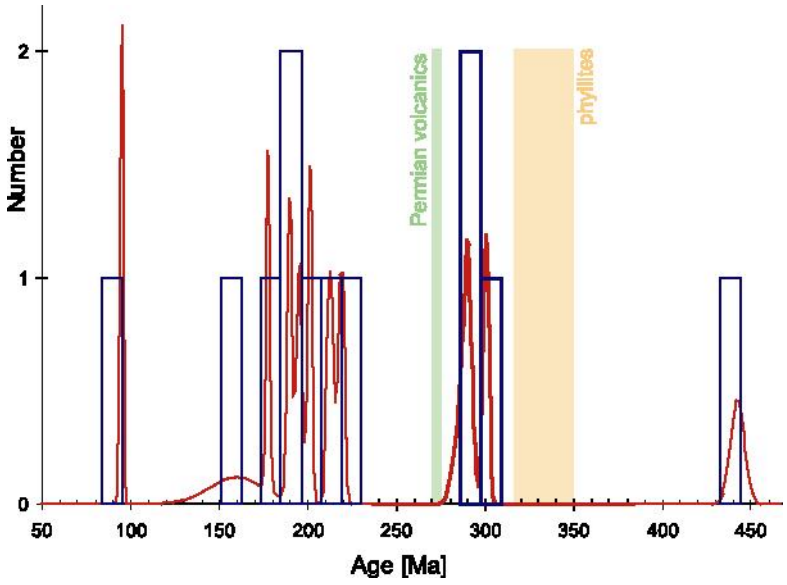

Fig. S2: Frequency (red line) and histogram (blue bars) diagram of $^{40}Ar/^{39}Ar$ ages of white micas from the intestine of the Iceman. The shaded bars indicate the range of ages for the Permian volcanics and phyllites, respectively. The distribution and range of ages is consistent only with the polymetamorphic gneiss lithology; the age at 442 Ma is attributed to excess-^{40}Ar, as such old white mica ages are not readily found in the area.

Supporting tables

Table S1a: $\delta^{18}O$ and $\delta^{13}C$ data of the Iceman's biominerals and 3rd molars of human teeth from the contemporaneous population. The last column ($\delta^{18}O_{ppt,\ SMOW}$) represents the oxygen isotopic composition of water calculated from enamel or bone that is inferred to have been ingested during biomineral formation. The latter value has been calculated after conversion between the PDB and SMOW scale using the following relationships: $\delta^{18}O_{apat,phos} = (\delta^{18}O_{ppt} \times 0.64) + 22.37$ (*S41*) and $\delta^{18}O_{apat,carb\ (SMOW)} = (\delta^{18}O_{phos} + 8.5) / 0.98$ (*S42*), with the following abbreviations: apat...apatite, phos...phosphate, ppt...precipitation, carb...carbonate; 3…canine, 4…1st premolar, lg…large.

Sample ID	Valley	Elevation (m)	Location (10º30' - 12º10' E) (46º10' - 47º20' N)	$\delta^{13}C_{apat,carb}$ (PDB)	$\delta^{18}O_{apat,carb}$ (PDB)	$\delta^{18}O_{ppt}$ (SMOW)
Iceman						
3, dental enamel		-	-	-13.76	-6.34	-10.98
4lg2, dental enamel		-	-	-13.60	-6.07	-10.56
Z2KN4a, trabecular bone		-	-	-15.26	-6.54	-11.31
Z2KN4b, trabecular bone		-	-	-15.22	-6.65	-11.48
Z2KN5a, cortical bone		-	-	-15.37	-6.75	-11.63
Z2KN5b, cortical bone		-	-	-15.21	-6.76	-11.66
3rd molars of modern humans						
MTS1	Eisack/Isarco	900	Feldthurns	-13.86	-5.87	-10.25
WRS1	Eisack/Isarco	750	Völs	-13.69	-5.87	-10.24
MTS2	Eisack/Isarco	1300	Ritten/Oberinn	-14.45	-6.23	-10.81
MTS14	Eisack/Isarco	1150	Klobenstein/Ritten	-13.76	-7.89	-13.43
MTS17	Eisack/Isarco	1060	Kastelruth	-13.95	-6.38	-11.05
MTS18	Eisack/Isarco	1150	Ratschings	-14.38	-6.26	-10.86
MTS23	Eisack/Isarco	970	Sarnthein	-13.51	-5.76	-10.08
MTS3	Etsch/Adige	450	Eppan	-13.78	-7.25	-12.42
MTS5	Etsch/Adige	260	Bozen	-14.22	-6.75	-11.64
MTS12	Etsch/Adige	400	Eppan	-13.82	-6.97	-11.98
MTS16	Etsch/Adige	1500	Reschen	-14.20	-8.20	-13.93
MTS19	Etsch/Adige	580	Rabland	-14.18	-7.07	-12.15
MTS20	Etsch/Adige	500	Riffian	-13.94	-7.20	-12.35
MTS21	Etsch/Adige	260	Bozen	-14.44	-5.29	-9.33
MTS22	Etsch/Adige	300	Lana	-13.76	-7.74	-13.19
MTS6	near Hohlen valley	1360	Deutschnofen	-13.80	-6.61	-11.41
MTS13	Rienz (Puster valley)	780	Mühlbach	-13.78	-6.96	-11.96
MTS15	Gröden valley	1240	St. Ulrich/Gröden	-13.96	-7.39	-12.65

Table S1b: $\delta^{18}O$ data of river water and corresponding local streams/springs located in Italy and Austria (Fig. 1), as well as of ice cores at the Iceman site (see (*S4*) for sample numbers and related information). Average $\delta^{18}O$ values of river water have been calculated from individual sampling campaigns in late June 2001, late September 2001 and early June 2002, using appropriate river runoff data supplied by Austrian and Italian authorities. Differences in $\delta^{18}O$ between June (influenced by snow melt) and September are <0.8 ‰, and for most stations <0.5 ‰. Abbreviations: I…Italy, A…Austria; v…valley. The subscript 's' denotes local springs and streams located in the respective valley.

SampleID	River / site (valley)	Locality (state) (10º30' - 12º10' E) (46º10' - 47º20' N)	Elevation (m)	$\delta^{18}O$ (SMOW)
Southern rivers/springs				
EI230	Eisack/Isarco	S Bozen/Bolzano (I)	234	-12.14
EI500	Eisack/Isarco	Klausen (I)	506	-12.20
EI750	Eisack/Isarco	Franzensfeste (I)	752	-12.19
EI1000	Eisack/Isarco	Gossensass (I)	1005	-12.37
EI1350	Eisack/Isarco	S Brenner Pass (I)	1348	-12.46
EI_s1	SW Barbian; local stream (Eisack v.)	Barbian (I)	950	-9.98
EI_s2	SW Barbian; local stream (Eisack v.)	Barbian (I)	955	-9.26
EI_s3	SW Barbian; local stream (Eisack v.)	Barbian (I)	960	-9.93
EI_s4	N Barbian; W St. Gertraud (Eisack v.)	Barbian (I)	870	-9.50
EI_s5	N Feldthurns; spring (Eisack v.)	Feldthurns (I)	900	-9.28
EI_s6	SW Feldthurns; local stream (Eisack v.)	Feldthurns (I)	900	-9.83
EI_s7	N Feldthurns; local stream (Eisack v.)	Feldthurns (I)	1050	-10.33
EI_s8	NW Villanders; local stream (Eisack v.)	Villanders (I)	1150	-9.50
EI_s9	NNW Villanders; local stream (Eisack v.)	Villanders (I)	1150	-9.68
EI_s10	Völserried; spring (Eisack v.)	Völs (I)	750	-9.18
GB	Gröden river (near confluence with Eisack/Isarco)	Waidbruck (I)	479	-11.63
RI660	Rienz (Puster valley)	Mühlbach (I)	658	-11.94
RI750	Rienz (Puster valley)	Niedervintl (I)	750	-12.34
RI1000	Rienz (Puster valley)	N Olang (I)	1000	-11.54
RI1200	Rienz (Puster valley)	E Niederdorf(I)	1200	-11.74
RI1220	Rienz (Puster valley)	SW Toblach (I)	1220	-11.54
RI_s1	Sonnenburg (Puster valley); spring	W Bruneck (I)	820	-10.94

SampleID	River / valley / site	Locality (state)	Elevation [m]	$\delta^{18}O$ (SMOW)
ET210	Etsch/Adige	San Michele (I)	215	-12.38
ET240	Etsch/Adige	S Terlan (I)	243	-12.87
ET500	Etsch/Adige	Töll (I)	500	-13.79
ET750	Etsch/Adige	Göflan, S Schlanders (I)	746	-14.00
ET1000	Etsch/Adige	Glurns (I)	955	-13.63
ET1500	Etsch/Adige	S Reschenpass (I)	1498	-13.77
ET_s1	Juval castle; spring (Etsch v.)	W Naturns (I)	925	-12.26
HO	Hohlen river (near confluence with Etsch/Adige)	Auer/Ora (I)	225	-10.87
LT1500	Langtaufers	Graun (I)	1520	-14.86
LT1900	Langtaufers	E Melag (I)	1935	-14.96
NO210	Non valley	Mezzocorona (I)	222	-11.72
NO500	Non valley	SE Cles (I)	533	-11.11
UT280	Ulten valley	Lana (I)	275	-12.00
UT750	Ulten valley	St. Pankratz (I)	735	-12.02
UT1000	Ulten valley	St. Walpurga (I)	1070	-12.20
UT1500	Ulten valley	St. Gertraud (I)	1464	-12.82
UT1900	Ulten valley	Weissbrunnersee (I)	1880	-12.56
ST500	Schnals valley	E Juval (I)	562	-13.09
ST1000	Schnals valley	W Katharinaberg (I)	1002	-13.28
ST1500	Schnals valley	Unser Frau (I)	1501	-13.67
ST2000	Schnals valley	Kurzras (I)	2002	-14.27
Northern rivers				
IN600	Inn	Innsbruck (A)	608	-14.40
IN750	Inn	Silz (A)	750	-14.57
IN1000	Inn	Pfunds (A)	990	-14.18
NR1500	Inn (tributary)	N Reschenpass (A)	1474	-14.54
RO	Rosanna (near confluence with Inn)	Landeck (A)	805	-14.58
OT700	Ötz valley	W Ötztal Bhf. (A)	700	-14.82
OT1000	Ötz valley	N Umhausen (A)	1024	-15.09
OT1500	Ötz valley	Zwieselstein (A)	1484	-14.95
OT1900	Ötz valley	Rofen, W Vent (A)	1950	-15.58

SampleID	River / valley / site	Locality (state)	Elevation [m]	$\delta^{18}O$ (SMOW)
WI600	Wipp valley	Innsbruck, Sillpark (A)	600	-13.83
WI1300	Wipp valley	Brennersee, N Brenner Pass (A)	1304	-13.15
WI1000	Wipp valley	Steinach/Brenner (A)	1028	-13.04
Ice cores				
92/247	Ice core, near Iceman's hat	Iceman site (*S4*)	3213	-16.24
92/61	Ice core, 2.5 m N Iceman, 34-50 cm depth	Iceman site (*S4*)	3213	-13.38

Table S2a: Sr isotopic and concentration data of samples related to the Iceman, as well as of ice cores and soil leachates. Sample weights and concentrations of biominerals include all corresponding leaching/dissolution steps per sample. The sample identifiers for bone, ice core and organic samples correspond to those in (*S2, S4*). Errors refer to the last digits and include both the error of individual measurement and the long-term reproducibility of the NIST SRM987 standard. Abbreviations: 3…canine, 4…1st premolar, 5…2nd premolar; sm…small, lg…large; en…enamel, de…dentine; L1...leach 1, L2…leach 2, D…dissolution step; intcont…intestine content, intwall…intestine wall, n.a…. not analyzed.

Sample ID	Sample weight [mg]	Sr conc. [ppm]	$^{87}Sr/^{86}Sr$ (± 95% c.l.)	Sr released [%] (cumulative)
Enamel:				
3sm_en L1	4.50	81.8	0.721058 ± 17	7.72
3sm_en L2			0.721309 ± 17	32.47
3sm_en D			0.721464 ± 17	100
3lg L1	9.17	93.4	0.719794 ± 19	5.30
3lg L2			0.720217 ± 20	23.39
3lg D			0.720280 ± 19	100
4lg1 L1	1.23	95.8	0.719992 ± 27	10.09
4lg1 L2			0.720257 ± 19	69.49
4lg1 D			0.720610 ± 19	100
5 L1	4.64	92.4	0.720028 ± 23	6.56
5 L2			0.720029 ± 19	33.41
5 D			0.720322 ± 19	100
Dentine:				
3sm_de L1	0.295	88.3	0.720684 ± 44	32.91
3sm_de L2			0.720633 ± 32	75.94
3sm_de D			0.720754 ± 51	100
Bone - cortical:				
Z2KN1 L1	6.02	83.1	0.718046 ± 20	18.67
Z2KN1 L2			0.718080 ± 18	64.87
Z2KN1 D			0.717468 ± 19	100
Z2KN2 L1	4.28	77.3	0.718507 ± 20	28.62
Z2KN2 L2			0.718529 ± 29	78.83
Z2KN2 D			0.718076 ± 22	100
Bone - trabecular:				
Z2KN3 L1	5.94	65.4	0.718934 ± 15	25.38
Z2KN3 L2			0.718625 ± 15	71.47
Z2KN3 D			0.718440 ± 18	100

Sample ID	Sample weight [mg]	Sr conc. [ppm]	$^{87}Sr/^{86}Sr$ (± 95% c.l.)	Sr released [%] (cumulative)
Intestine				
intcont	2.20	0.363	0.71941 ± 27	---
intwall	5.63	0.196	0.72136 ± 20	---
Ice cores				
92/61 34-50 cm	----	n.a.	0.720097 ± 42	---
92/247 near hat	----	n.a.	0.722775 ± 81	---
92/379 under hat	6620	0.00783	0.727044 ± 18	---
92/152 near legs	5360	0.00177	0.728806 ± 48	---
92/171 bow	6780	0.00069	0.717426 ± 121	---
92/68 under quiver	5990	0.00111	0.722476 ± 151	---
Equipment + clothing				
92/400 larch	9.98	2.02	0.729055 ± 45	---
92/402b lime bast	9.51	1.71	0.719022 ± 24	---
UF:0/1 fur	19.09	1.51	0.729375 ± 20	---
UF:0/2 fur	16.06	7.54	0.721445 ± 15	---
Soil leachates				
BA1L	----	n.a.	0.723098 ± 14	---
MT1L	----	n.a.	0.710033 ± 14	---
IS1L	----	n.a.	0.705278 ± 14	---
IS2L	----	n.a.	0.707531 ± 55	---
JU1L	----	n.a.	0.721855 ± 14	---
JU2L	----	n.a.	0.720874 ± 20	---
KA1L	----	n.a.	0.720640 ± 14	---
KA2L	----	n.a.	0.720985 ± 14	---
PK1L	----	n.a.	0.719092 ± 16	---
PK2L	----	n.a.	0.719354 ± 20	---
PK3L	----	n.a.	0.717633 ± 16	---
VE1L	----	n.a.	0.720130 ± 14	---
VE2L	----	n.a.	0.720423 ± 14	---
VE3L	----	n.a.	0.720308 ± 14	---
VP1L	----	n.a.	0.723788 ± 26	---
VP2L	----	n.a.	0.723446 ± 17	---
VS1L	----	n.a.	0.713632 ± 15	---
VS2L	----	n.a.	0.712761 ± 14	---

Table S2b: Pb isotopic data of the Iceman's biominerals and soil leachates. Concentrations of biominerals include the leaching/dissolution steps indicated only. The sample identifiers for bone, ice core and organic samples correspond to those in (*S2, S4*). Errors refer to the last digits and include both the error of individual measurement and the long-term reproducibility of the NIST SRM981 standard. Abbreviations: 3…canine, 5…2nd premolar; L2…leach 2, D…dissolution step; en…enamel, cort…cortical, trab…trabecular, n.a…. not analyzed.

SampleID	Pb conc. [ppm]	$^{208}Pb/^{206}Pb$ (± 95% c.l.)	$^{207}Pb/^{206}Pb$ (± 95% c.l.)	$^{206}Pb/^{204}Pb$ (± 95% c.l.)
Enamel				
3lg5 D	0.12	2.0894 ± 31	0.84842 ± 76	18.597 ± 57
Bones				
Z2KN1 L2+D (cort.)	0.41	2.1145 ± 31	0.86139 ± 70	18.298 ± 55
Z2KN2 L2+D (cort.)	0.59	2.1015 ± 31	0.85199 ± 73	18.509 ± 57
Z2KN3 D (trab.)	0.49	2.0855 ± 52	0.84577 ± 161	18.594 ± 64
Soil leachates				
BA1L	n.a.	2.10299 ± 14	0.849828 ± 31	18.4525 ± 18
MT1L	n.a.	1.97616 ± 16	0.806172 ± 36	19.4977 ± 21
IS1 L	n.a.	2.06582 ± 23	0.837264 ± 55	18.7195 ± 115
IS2 L	n.a.	2.05631 ± 19	0.831583 ± 46	18.8769 ± 32
JU1L	n.a.	2.09301 ± 14	0.853554 ± 31	18.3372 ± 18
JU2L	n.a.	2.10006 ± 14	0.857553 ± 30	18.2372 ± 17
KA1L	n.a.	2.09547 ± 14	0.852984 ± 32	18.3446 ± 17
KA2L	n.a.	2.09218 ± 14	0.849957 ± 31	18.4266 ± 17
PK1L	n.a.	2.07281 ± 27	0.834187 ± 61	18.8109 ± 54
PK2L	n.a.	2.07364 ± 19	0.836417 ± 43	18.7622 ± 32
PK3L	n.a.	2.09998 ± 14	0.853737 ± 31	18.3452 ± 18
VE1L	n.a.	2.09977 ± 22	0.849690 ± 49	18.4674 ± 38
VE2L	n.a.	2.09985 ± 15	0.849096 ± 35	18.4741 ± 19
VE3L	n.a.	2.09733 ± 15	0.847987 ± 33	18.5068 ± 21
VP1L	n.a.	2.10895 ± 14	0.858102 ± 31	18.2662 ± 17
VP2L	n.a.	2.10879 ± 14	0.858077 ± 31	18.2649 ± 18
VS1L	n.a.	2.09209 ± 14	0.848180 ± 30	18.4798 ± 19
VS2L	n.a.	2.08486 ± 16	0.842207 ± 35	18.6292 ± 25

Tab. S3: $^{40}Ar/^{39}Ar$ isotopic data of white micas from the Iceman's intestine.

Grain number	Grain size (µm)	Comments	Age (Ma)	+-	$^{40}Ar^*/^{39}Ar$	+-	$^{40}Ar/^{39}Ar$	+-	$^{38}Ar/^{39}Ar$	+-	$^{37}Ar/^{39}Ar$	+-	$^{36}Ar/^{39}Ar$	+-	^{39}Ar (cm^3)	+-
Grain 10	295 x 251	Biotite or badly stained white mica	442.24	3.98	60.40	0.53	74.50	0.53	0.02628	0.00019	0.05537	0.01567	0.04771	0.00111	1.28E-12	9.09E-15
Grain 7	231 x 209	Slightly stained white mica	300.32	1.53	39.38	0.09	39.82	0.09	0.01101	0.00082	0.00523	0.00384	0.00147	0.00000	3.68E-12	8.57E-15
Grain 9	269 x 145	Biotite or badly stained white mica	290.49	2.06	37.99	0.22	48.57	0.15	0.05841	0.00127	0.02684	0.00880	0.03581	0.00064	2.16E-12	6.78E-15
Grain 3	376 x 217	White mica + biotite/ badly stained patch	286.91	4.07	37.48	0.54	38.88	0.50	0.01226	0.00061	0.01385	0.00137	0.00475	0.00084	4.57E-12	5.69E-14
Grain 11	395 x 257	Slightly stained white mica	218.78	1.67	28.03	0.18	29.56	0.18	0.01327	0.00037	0.01949	0.00119	0.00517	0.00018	7.59E-12	4.61E-14
Grain 2	151 x 178	Clean white mica	212.65	1.78	27.20	0.20	27.76	0.08	0.01423	0.00003	0.01023	0.00144	0.00188	0.00063	2.16E-12	3.83E-15
Grain 1	345 x 231	Clean white mica	201.24	1.18	25.66	0.09	26.06	0.05	0.01171	0.00002	0.00440	0.00062	0.00135	0.00027	5.02E-12	8.57E-15
Grain 5	352 x 229	Clean white mica	195.16	1.70	24.84	0.19	25.10	0.02	0.01309	0.00001	0.00273	0.00000	0.00086	0.00064	4.70E-12	3.03E-15
Grain 6	337 x 172	Clean white mica	189.47	1.29	24.08	0.12	24.08	0.04	0.01389	0.00002	0.00750	0.00184	0.00000	0.00000	3.42E-12	5.59E-15
Grain 4	172 x 139	Clean white mica	177.69	1.00	22.51	0.07	22.51	0.07	0.01568	0.00005	0.03545	0.00011	0.00000	0.00000	8.93E-13	2.71E-15
Grain 12	166 x 111	Clean white mica	160.11	15.35	20.18	2.02	26.20	0.20	0.01407	0.00010	0.17816	0.01598	0.02039	0.00681	3.98E-13	2.71E-15
Grain 8	161 x 85	Moderately stained white mica	94.69	0.81	11.72	0.08	15.44	0.10	0.01518	0.00210	0.02987	0.01960	0.01259	0.00007	6.45E-13	3.83E-15
J value = 0.004599 ± 0.000023																
1 sigma errors																
Age standard used = Tinto B biotite (409.24 ± 0.71 Ma).																

Supporting references

S1. G. Bonani, S. D. Ivy, I. Hajdas, T. R. Niklaus, M. Suter, *Radiocarbon* **36**, 247-250 (1994).

S2. R. Prinoth-Fornwagner, T. R. Niklaus, *Nuclear Instruments & Methods in Physics Research Section B- Beam Interactions with Materials and Atoms* **92**, 282-290 (1994).

S3. K. Oeggl, W. Schoch, in *The Iceman and his Natural Environment* S. Bortenschlager, K. Oeggl, Eds. (Springer, Wien, New York, 2000), vol. 4, pp. 29-61.

S4. B. Bagolini, L. Dal Ri, A. Lippert, H. Nothdurfter, in *Der Mann im Eis - Neue Funde und Ergebnisse* K. Spindler, E. Rastbichler-Zissernig, H. Wilfling, D. zur Nedden, H. Nothdurfter, Eds. (Springer, Wien, New York, 1995), vol. 2, pp. 3-22.

S5. A. Fleckinger, H. Steiner, *The fascination of the Neolithic Age - The Iceman* (Folio, Bolzano, Vienna, 1999).

S6. W. Müller, (unpublished data).

S7. S. Eggins, R. Grün, A. W. G. Pike, J. M. G. Shelley, L. Taylor, *Quaternary Science Reviews* **22**, 1373-1382 (2003).

S8. P. Horn, S. Hölzl, D. Storzer, *Naturwissenschaften* **81**, 360-362 (1994).

S9. E. P. Horwitz, R. Chiarizia, M. L. Dietz, *Solvent Extraction and Ion Exchange* **10**, 313-336 (1992).

S10. N. Vajda, J. LaRosa, R. Zeisler, P. Danesi, G. Kis-Benedek, *Journal of Environmental Radioactivity* **37**, 355-372 (1997).

S11. R. J. Theriault, W. J. Davis, in *Radiogenic Age and Isotopic Studies*. (Geological Survey of Canada, 2000), vol. 13, pp. 3.

S12. W. Müller, D. Aerden, A. N. Halliday, *Science* **288**, 2195-2198 (2000).

S13. H. Gerstenberger, G. Haase, *Chemical Geology* **136**, 309-312 (1997).

S14. S. J. G. Galer, W. Abouchami, *Mineralogical Magazine* **62A**, 491-492 (1998).

S15. R. H. Steiger, E. Jäger, *Earth and Planetary Science Letters* **36**, 359-362 (1977).

S16. D. C. Rex, P. G. Guise, in *Phanerozoic Time Scale, International Geological Correlation Programme* G. S. Odin, Ed. (Paris, 1995), vol. 13, pp. 21-23.

S17. J. C. Hess, H. J. Lippolt, in *Phanerozoic Time Scale, International Geological Correlation Programme* G. S. Odin, Ed. (Paris, 1994), vol. 12, pp. 19-23.

S18. I. McDougall, T. M. Harrison, *Geochronology and thermochronology by the $^{40}Ar/^{39}Ar$ method* (Oxford University Press, New York, 2nd ed, 1999).

S19. S. P. Kelley, in *Microprobe techniques in the earth sciences* P. J. Potts, Bowles, J. F. W., Reed, S. J. B., Cave, M. R., Ed. (Chapman & Hall, London, 1995), vol. 6, pp. 123-143.

S20. B. Luz, Y. Kolodny, M. Horowitz, *Geochimica Et Cosmochimica Acta* **48**, 1689-1693 (1984).

S21. K. Oeggl, J. H. Dickson, S. Bortenschlager, in *The Iceman and his Natural Environment* S. Bortenschlager, K. Oeggl, Eds. (Springer, Wien, New York, 2000), vol. 4, pp. 163-166.

S22. M. A. Pabst, F. Hofer, *American Journal of Physical Anthropology* **107**, 1-12 (1998).

S23. J. Hoogewerff *et al.*, *Journal of Archaeological Science* **28**, 983-989 (2001).

S24. C. Kralik, W. Kiesl, H. Seidler, W. Platzer, W. Rabl, in *Human Mummies* K. Spindler, H. Wilfling, E. Rastbichler-Zissernig, D. zur Nedden, H. Nothdurfter, Eds. (Springer, Wien, New York, 1996), vol. 3, pp. 283-287.

S25. R. E. M. Hedges, *Archaeometry* **44**, 319 - 328 (2002).

S26. G. Bigi, D. Cosentino, M. Parotto, R. Sartori, P. Scandone. (CNR Italy, Firenze, 1990).

S27. S. Borsi, A. Del Moro, G. Ferrara, *Bolletino della Societa Geologica Italiana* **91**, 387-406 (1972).
S28. S. Borsi, A. Del Moro, F. P. Sassi, A. Zanferrari, G. Zirpoli, *Memorie di Scienze Geologiche* **32**, 1-17 (1978).
S29. M. Thöni, *Mitteilungen der österreichischen geologischen Gesellschaft* **71/72**, 139-165 (1980).
S30. M. Thöni, *Jahrbuch der Geologischen Bundesanstalt Wien* **124**, 111-174 (1981).
S31. A. Del Moro, D. Visona, *Neues Jahrbuch Für Mineralogie-Abhandlungen* **145**, 66-85 (1982).
S32. A. Del Moro, G. Pardini, C. Quercioli, I. M. Villa, E. Callegari, *Memorie della Societa Geologica Italiana* **26**, 285-299 (1983).
S33. M. Thöni, G. Hoinkes, *Memorie di Scienze Geologiche* **36**, 211-238 (1983).
S34. F. P. Sassi, G. Cavazzini, D. Visona, *Rendiconti della Societa Italiana di Mineralogia e Petrologia* **40**, 187-224 (1985).
S35. K. Hammerschmidt, B. Stöckhert, *Contributions to Mineralogy and Petrology* **95**, 393-406 (1987).
S36. S. Barth, F. Oberli, M. Meier, *Earth and Planetary Science Letters* **95** (1989).
S37. S. Barth, F. Oberli, M. Meier, *Earth and Planetary Science Letters* **124**, 149-159 (1994).
S38. R. Spiess, *Schweizerische Mineralogische Und Petrographische Mitteilungen* **75**, 413-425 (1995).
S39. M. Thöni, *Schweizerische Mineralogische Und Petrographische Mitteilungen* **79**, 209-230 (1999).
S40. R. Spiess, M. Marini, W. Frank, B. Marcolongo, G. Cavazzini, *Schweizerische Mineralogische Und Petrographische Mitteilungen* **81**, 1-16 (2001).
S41. A. Longinelli, *Geochimica Et Cosmochimica Acta* **48**, 385-390 (1984).
S42. P. Iacumin, H. Bocherens, A. Mariotti, A. Longinelli, *Earth and Planetary Science Letters* **142**, 1-6 (1996).